Carcinogenesis vol.34 no.3 pp.550–559, 2013
doi:10.1093/carcin/bgs375
Advance Access publication December 7, 2012

Cathepsin B and uPAR regulate self-renewal of glioma-initiating cells through GLI-regulated Sox2 and Bmi1 expression

Sreelatha Gopinath[1], RamaRao Malla[1], Kiranmai Alapati[1], Bharathi Gorantla[1], Meena Gujrati[2], Dzung H.Dinh[3] and Jasti S.Rao[1,3,*]

[1]Department of Cancer Biology & Pharmacology, [2]Department of Pathology and [3]Department of Neurosurgery, University of Illinois College of Medicine at Peoria, One Illini Drive, Peoria, IL 61656, USA

*To whom correspondence should be addressed. Department of Cancer Biology and Pharmacology, University of Illinois College of Medicine, Box 1649, Peoria, IL 61656, USA. Tel: +309 671 3445; Fax: 309 671 3442; Email: jsrao@uic.edu

Cancer-initiating cells comprise a heterogeneous population of undifferentiated cells with the capacity for self-renewal and high proliferative potential. We investigated the role of uPAR and cathepsin B in the maintenance of stem cell nature in glioma-initiating cells (GICs). Simultaneous knockdown of uPAR and cathepsin B significantly reduced the expression of CD133, Nestin, Sox2 and Bmi1 at the protein level and GLI1 and GLI2 at the messenger RNA level. Also, knockdown of uPAR and cathepsin B resulted in a reduction in the number of GICs as well as sphere size. These changes are mediated by Sox2 and Bmi1, downstream of hedgehog signaling. Addition of cyclopamine reduced the expression of Sox2 and Bmi1 along with GLI1 and GLI2 expression, induced differentiation and reduced subsphere formation of GICs thereby indicating that hedgehog signaling acts upstream of Sox2 and Bmi1. Further confirmation was obtained from increased luciferase expression under the control of a GLI-bound Sox2 and Bmi1 luciferase promoter. Simultaneous knockdown of uPAR and cathepsin B also reduced the expression of Nestin Sox2 and Bmi1 *in vivo*. Thus, our study highlights the importance of uPAR and cathepsin B in the regulation of malignant stem cell self-renewal through hedgehog components, Bmi1 and Sox2.

Introduction

Glioblastoma (GBM) is the most frequent and most aggressive type of primary brain tumor in humans (1) and, even in the most favorable cases, patients with malignant glioma die within 2 years (2). Standard therapies are not successful because of the infiltrative behavior of the tumor cells. Recurrence of the tumor is now attributed to a small population of cells termed cancer-initiating cells/cancer stem cells (3–5). Stem cells are characterized by their ability to self-renew as well as to generate differentiated cells within each organ. Most of the recent work being carried out is focused on targeting the self-renewal capacity of cancer stem cells. A number of developmental signaling pathways, such as Wnt, Notch and hedgehog, have been found to play a role in regulating the self-renewal of normal stem cells in the hematopoietic system, the skin, the nervous system and the breast (6–8). A series of pathways, including sonic hedgehog (SHH), Notch and Wnt-β-catenin, have been shown to be implicated in the resistance of gliomas to alkylating agents and/or the maintenance of brain tumor stem cells. Apart from these signaling events, transcription factors, such as Sox2 and Bmi1, have been extensively studied due to their role in cancer stem cell initiation and maintenance of various cancer stem cells (9–11).

SHH is involved in prenatal brain development and is associated with cell proliferation. The SHH pathway is active in brain tumors and its inhibition by cyclopamine decreases the proliferation of brain tumor cells (12). The importance of this pathway in the maintenance of glioma progenitor cells has been reported previously (13,14). Clement *et al.* (13). showed that SHH signaling regulates the expression of 'stemness' genes and the self-renewal of CD133-expressing (CD133+) glioma cancer stem cells.

The transcription factor Sox2 is considered a master gene of mammalian embryogenesis and plays a pivotal role in sustaining growth and self-renewal of several stem cell types, both embryonic and adult (15–17). Sox2 has also been implicated in several cancers including glioma (18–20), gastric cancer (21), breast cancer (22) and pancreatic cancer (23). Sox2 deficiency causes impaired neurogenesis in adult mouse brain (24). The transcription factor Sox2 controls gene expression during development and has roles in both neurogenesis and gliogenesis; a positive correlation between Sox2 expression and malignancy grade in gliomas has been reported (25). Bmi1, a member of the polycomb group proteins, is involved in brain development (26), and it is amplified and/or overexpressed in various human cancers, such as non-small cell lung cancer (27), colorectal carcinoma (28), medulloblastoma (26), lymphoma (29), multiple myeloma (30) and primary neuroblastoma (31). In addition, it was recently shown that inhibition of Bmi1 by microRNA-128 attenuates glioma cell proliferation and self-renewal (32). Mice lacking Bmi1 display neurological abnormalities and postnatal depletion of stem cells from the central and peripheral nervous systems (33–36). Importantly, the *INK4A/ARF* locus, which encodes the two tumor suppressor proteins p16INK4A and p14ARF, is the main target of Bmi1 oncogenic and stem cell proliferation activities (37).

Here, we report that upregulation of uPAR and cathepsin B induces Sox2 and Bmi1 expression, which play essential roles in the maintenance of the stemness of glioma-initiating cells (GICs). Further, short hairpin RNA (shRNA) targeted against uPAR and cathepsin B reduced the expression of Sox2 and Bmi1. We also demonstrate that GLI2, a key mediator of SHH signaling, acts upstream of Sox2 and Bmi1 and influences their expression by binding to the promoter. These findings open the way to deprive glioma stem cells (GSCs) of their tumorigenic activity and will offer new therapeutic possibilities.

Materials and methods

Cell culture

Glioma cell lines U87 and U251 were used in this study. For wild-type and the CD133− cells, we used Dulbecco's modified Eagle's medium (DMEM) with 10% fetal bovine serum and 1% penicillin/streptomycin. For isolated CD133+ cells, we used serum-free DMEM F12 50/50 containing recombinant human epidermal growth factor (20 ng/ml), basic fibroblast growth factor (20 ng/ml), leukemia inhibitor factor (10 ng/ml) and N2 supplements.

Isolation of CD133+ cells

Evaluation of the size of the CD133+ population in each cell line was undertaken by flow cytometry using a phycoerythrin- (PE) labeled antibody, CD133/1 (clone AC133/1; Miltenyi Biotec, Bergisch Gladbach, Germany). Cells grown in Petri plates were washed once with sterile 1× phosphate-buffered saline (PBS), detached and centrifuged. The pellet was blocked in filter-sterilized 2% bovine serum albumin in PBS for 30 min. Then, the cells were incubated with PE-labeled CD133 antibody (1:100 in 1% bovine serum albumin) for 30 min at 4°C. An isotype- and concentration-matched PE-labeled control IgG antibody (Miltenyi Biotec) was used, and samples labeled with this antibody were used to set the gating levels. After three 5 min washes with 1× PBS, the cells were used for sorting CD133+/CD133− cells. Sorting was performed on FACSAria (BD Biosciences), and the data were analyzed. Sorted

Abbreviations: DAPI, 4′,6-diamidino-2-phenylindole; DMEM, Dulbecco's modified Eagle's medium; FACS, fluorescence-activated cell sorting; GAPDH, glyceraldehyde 3-phosphate dehydrogenase; GBM, glioblastoma; GICs, glioma-initiating cells; mRNA, messenger RNA; PBS, phosphate-buffered saline; PE, phycoerythrin; SHH, sonic hedgehog; shRNA, short hairpin RNA; siRNA, small interfering RNA; SV, scrambled vector.

CD133+ cells were cultured in DMEM F12 50/50 with added growth factors, and the CD133− cells were cultured in serum-containing DMEM. U87 and U251 CD133+ cells were labeled as U87S and U251S, respectively. Similarly, CD133−ve cells were labeled as U87NS and U251NS, respectively.

Subsphere formation and differentiation assays

The isolated CD133+ cells were maintained in the neural stem cell medium as described earlier, and when the primary spheres reached an approximate size of 100–200 cells per sphere, they were dissociated and plated onto a 96-well plate containing 0.1 ml of neural stem cell medium at 1–2 cells per well. Adherent non-sphere forming cells and parental cells were used as controls when determining capacity to form tumor cell clones. Cells were maintained in the plate for 14 days, and fresh medium was added every 2–3 days. Then, the wells were scored for sphere formation and only those wells containing a single cell were considered. Spheres that were developed in the 96-well plates were dissociated into single cell suspension and seeded into chamber slides for differentiation assay. The cells were grown for 14 days in medium devoid of growth factors but permissive for differentiation. After the incubation period, the cells were subjected to immunofluorescence assay.

Transfections, radiation and inhibitor treatments

We used a bicistronic shRNA construct directed against both uPAR and cathepsin B (pCU) in this study. Construction of the bicistronic vector has been described previously (38). Small interfering RNA (siRNA) for Sox2 (Sox2-si) and Bmi1 (Bmi-si) were purchased from Santa Cruz Biotechnology (Santa Cruz, CA). Full-length cathepsin B and uPAR overexpressing plasmids were purchased from Origene (Rockville, MD). All the antibodies used in this study were purchased from Santa Cruz Biotechnology unless otherwise specified. The scrambled vector (SV) sequence corresponded to the bicistronic shRNA directed against the cathepsin B and uPAR (pCU). The vectors were transfected into U87 and U251 wild-type cells as well as GICs independently with FuGene HD reagent as per the manufacturer's instructions (Roche Diagnostics, Indianapolis, IN). For GICs, sphere cells were dissociated before transfection. For the inhibitor study, cells seeded in six-well plates were treated with cyclopamine (10 µM), a potent hedgehog signaling inhibitor, for 24 h. To determine the chemoresistance of isolated U87S and U251S cells, we used temozolomide (10 µM). For radiation treatment, cells were irradiated with different doses of radiation (3, 5 and 10 Gy) using a RS 2000 Biological Irradiator (Rad Source Technologies, Boca Raton, FL).

Western blot and immunofluorescence assay

Cells were washed with ice-cold PBS and resuspended in radioimmune precipitation assay buffer. The cell lysates were analyzed by sodium dodecyl sulfate–polyacrylamide gel electrophoresis followed by western blotting. The following antibodies were used: uPAR, cathepsin B (Athens Research and Technology, Athens, GA), CD133, GFAP, Sox2, Bmi1, GLI1, Nestin and glyceraldehyde 3-phosphate dehydrogenase (GAPDH). Signals were detected using Pierce Western Blotting substrate (Pierce, Rockford, IL).

To determine the expression of neural stem cell (NSC) markers and lineage markers, we carried out immunostaining. For staining the primary cultured tumor cells and differentiated GBM spheres, the cells growing in pre-coated chamber slides were washed with PBS, fixed with 4% paraformaldehyde, permeabilized with ice-cold methanol and rehydrated with PBS. Anti-goat serum was used for blocking as well as for primary antibody dilution and incubation. The antibodies used in this study were CD133, Nestin, GFAP and β III tubulin. The cells were counterstained with 4′,6-diamidino-2-phenylindole (DAPI; Sigma) to reveal nuclei. Expression was visualized by fluorescence microscopy (Olympus IX71; Olympus Optical Co., Tokyo, Japan) and photographed.

Reverse transcription–PCR analysis

CD133+ spheres, wild-type cells, CD133− cells and all of the treated cells (transfection/inhibitors) and differentiated progeny were, respectively, subjected to total RNA extraction using Trizol reagent (Invitrogen, Carlsbad, CA) and converted to complementary DNA using Transcriptor First Strand cDNA synthesis kit (Roche Diagnostics) as per the manufacturer's instructions. Primers used for the study are listed in Supplementary Table 1, available at *Carcinogenesis* Online. GAPDH served as an internal control. PCR product was analyzed by agarose gel electrophoresis. Quantitative PCR analysis was set up with iQ SYBR Green Supermix kit (Bio-Rad Hercules, CA).

Chromatin immunoprecipitation analysis

Cytoplasmic and nuclear extracts from the treated cells were isolated using the Active Motif Nuclear Extraction Kit (Active Motif, Carlsbad, CA) according to the manufacturer's instructions. Nuclear fractions were subjected to chromatin immunoprecipitation analysis. GLI immunoprecipitations were performed, and the co-precipitated chromatin was analyzed by PCR for GLI recruitment on Sox2 and Bmi1 promoter using primers specific for Sox2 and Bmi1 promoters. Primers are listed in Supplementary Table 1, available at *Carcinogenesis* Online.

PGL3 promoter vector construction and luciferase assay

We constructed various PGL3 promoter constructs, including pGL3-Bmi1 luc, pGL3-Sox2 luc and pGL3-GLI2 luc vectors. Bmi1, Sox2 and GLI2 promoter regions were amplified from genomic DNA using the following primers with specified restriction sites on 5′ and 3′ regions of forward and reverse primers, respectively:

Bmi1-F: gtc**GAGCTC**GAGCATGGCTTTGAAAATGTC (*Sac*II site in bold)
Bmi1-R: gca**AGATCT**TGGGCAGTATCTTTCCCTCTT (*Bgl*II site in bold)
Sox2-F: gtc**GAGCTC**GGCTTTGTTTGACTCCGTGT (*Sac*II site in Bold)
Sox2-R: gca**AGATCT**GGGGCTGTCAGGGAATAAAT (*Bgl*II site in Bold)
GLI2-F: aaa**CTCGAG**CATGCACCAAATCCATAGAG (*Xho*I site in bold)
GLI2-R: aaa**AAGCTT**TCAGAGCAGAATGAGCGAAT (*Hind*III site in bold)

These primers amplify a 778 bp (located between −1880 to −1022 bp), a 1483 bp (located between −1501 to −18 bp) region and a 2 kb (located between −2080 to −80 bp), respectively. The PCR product was cloned into the promoter-less luciferase reporter vector, pGL3 basic (Promega, Madison, WI), predigested with respective enzymes and labeled as B1-luc for Bmi-luc promoter, S1-luc for Sox2-luc promoter and GLI2-luc for GLI2-luc promoter.

Luciferase activity was measured with Promega's luciferase assay kit. Following 48 h of transfection, cells were washed twice with PBS and lysed with 100 ml of reporter lysis buffer. The lysate was shaken at room temperature for 10 ± 15 min, after which 20 µl of each cell lysate was mixed with 100 µl of buffer and measured for luciferase activity in a Turner Luminometer (Turner Designs, Sunnyvale, CA) over an integration period of 15 s. Values obtained were normalized to GAPDH levels.

Tumor cell implantation, treatments and immunohistochemistry

Dissociated secondary sphere CD133+ cells/wild-type/CD133− cells were injected either subcutaneously (1×10^3cells) or orthotopically (1×10^5 cells) into the brains of 5-week-old female nude mice ($n = 5$ each). Mice with intracranially injected cells were treated with mock, SV and pCU using Alzet minipumps at the rate of 0.25 ml/h. After 4 (subcutaneous) and 6 weeks (intracranial) of cell implantation, animals were killed and tumors were processed. U251 GICs stably transfected with a luciferin-expressing plasmid were used to check the tumor formation efficiency and also for serial implantation studies ($n = 3$). Orthotopic tumor formation ability was also tested by implanting 100 CD133+ cells in matrigel. To detect tumor growth, animals received an intraperitoneal injection of 2.5 mg of D-luciferin sodium salt (Gold Biotechnology, St Louis, MO) suspended in 50 µl of PBS, and tumor growth was monitored using the IVIS-200 Xenogen imaging system (Xenogen Corporation, Alameda, CA). Brain sections were stained with hematoxylin and eosin to visualize tumor cells and to determine tumor volume. All of these procedures were carried out as described previously (39,40). To characterize the brain tissue using immunohistochemistry, sections were treated with primary antibodies for uPAR, cathepsin B, Nestin, Sox2 and Bmi1.

Results

Isolation and characterization of glioma stem cells

Increasingly, studies have shown that brain tumors originate from CD133+ cancer stem-like cells that recapitulate the self-renewal and multilineage differentiation characteristics of the original tumor (3,4,41). Through fluorescence-activated cell sorting (FACS), we obtained about 18–20% CD133+ cells in both the cell lines used (Figure 1A). Isolated CD133+ cells, after 3–4 generations, were further subjected to FACS analysis to check for CD133 expression; the results indicated 98% expression as compared with controls (Figure 1B). They were maintained under serum-free conditions and their ability to self-renew was assessed by the subsphere forming capacity of these cells (Supplementary Figure 1, available at *Carcinogenesis* Online). We compared the expression of stem cell markers in the CD133+ cells of both the cell lines. Total proteins isolated when subjected to immunoblot analysis revealed high expression of stem cell markers, such as Nestin and CD133, as compared with wild-type cells (Figure 1C). Further confirmation of the high expression of stem cell markers was obtained from immunocyto analysis (Figure 1D). To test the efficiency of stem cells to differentiate under serum

conditions, we dissociated the stem cell spheres, cultured them in serum medium for 7 days and immunostained them to determine the expression of differentiation markers. The results indicated that the cells efficiently differentiated in serum and showed high expression of GFAP, Tuj-I and O4 (Figure 1D). The immunogenicity of the cells was tested by injecting the CD133+, CD133− and wild-type cells (1×10^3) subcutaneously into the mice. CD133+ cells induced tumor formation within 1 month of injection, whereas the wild-type cells showed no signs of tumor formation. However, upon longer exposure (2 months), wild-type cells injected mouse formed small tumors (data not shown) indicating that the CD133+ cells are more tumorigenic as compared with the wild-type cells. CD133− cells failed to form tumors with the number of injected cells within the stipulated time period (Figure 1E). To test the orthotopic tumor initiation capacity of GICs, mice were injected with 100 CD133+ U251 luciferase cells and a serial *in vivo* transplantation study was also performed. Results indicated that within the stipulated time frame 100 CD133+ cells were sufficient to initiate tumors in mice (Supplementary Figure 2A, available at *Carcinogenesis* Online). Bioluminescence imaging of mice and hematoxylin and eosin staining after serial transplantation of cells showed tumor formation (Supplementary Figure 2B, available at *Carcinogenesis* Online). Also, we confirmed the stemness of the cells by exposing the cells to temozolamide and radiation. Both the treatments demonstrated the resistance of isolated CD133+ cells compared with the wild-type cells (Figure 1F).

uPAR and cathepsin B are highly expressed in glioma stem cells

As we have previously reported the importance of uPAR and cathepsin B expression in gliomas, we checked for the expression of uPAR and cathepsin B in glioma stem cells. Immunoblot results show that CD133+ cells had high expression levels of uPAR and cathepsin B when compared with the wild-type cells, indicating that these proteins might play a key role in maintaining the stemness of the CD133+ cells (Figure 2A). To test the potential roles of uPAR and cathepsin B in GICs, we first examined the effect of downregulation and upregulation of these two proteins on the biological characteristics. Immunoblot and reverse

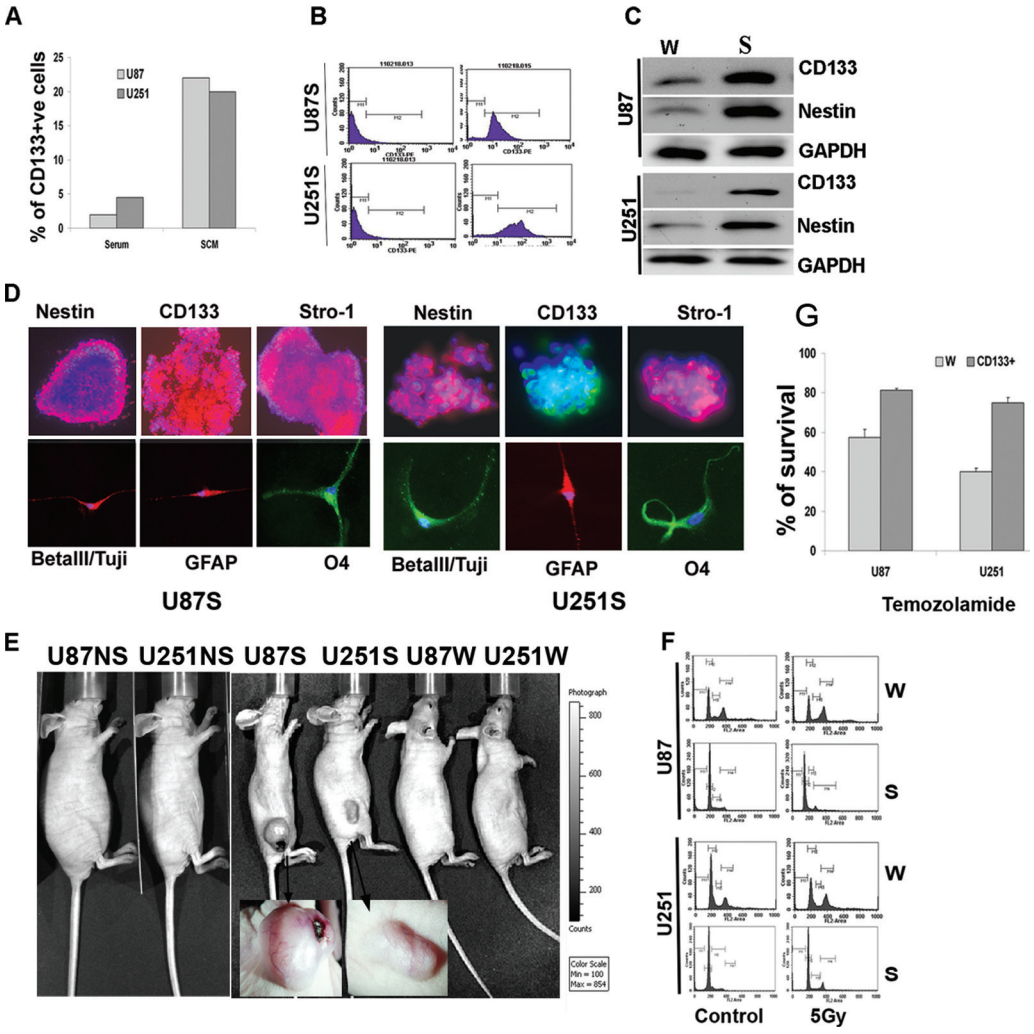

Fig. 1. Characterization of GICs from U87 and U251. (**A**) Graphical representation of percent of CD133+ cells obtained by FACS sorting using PE-conjugated CD133 antibody in U87 and U251 cells grown in serum-containing DMEM (serum) and DMEM F12 50/50 with added growth factors that allow stem cell enrichment. (**B**) After maintaining cells for 3–4 generations, isolated CD133+ cells from U87 and U251 were tested for CD133 expression by FACS analysis; the histograms are shown. (**C**) Immunoblot analysis of total cell lysates isolated from U87S and U251S cells and the wild-type cells of U87 and U251. Expression levels of CD133 and Nestin were checked by loading equal amounts of total protein. GAPDH was used as a loading control. (**D**) The expression of stem cell markers and multipotency of secondary sphere cell differentiation of U87 and U251 under confocal microscope. Spheres were fixed and immunostained with Nestin, CD133 and Stro-1. Multilineage capacity was assessed after growing the dissociated sphere cells in serum media for 7 days and then immunostained for Tuji, GFAP and O4 differentiation markers. DAPI was used for nuclear staining. Overlapped pictures of DAPI and the antibody are represented. (**E**) Tumorigenic capacity of U87S, U251S, U87W and U251W cells after injecting 1×10^3 cells subcutaneously. After 1 month, pictures of mice bearing tumors were photographed and are represented. (**F**) Radiation and chemo resistance of U87S, U251S, U87W and U251W cells were compared. Results of FACS analysis of the cells after radiation (5 Gy) are shown. (**G**) Graphical representation of percentage of survival of cells exposed to temozolomide.

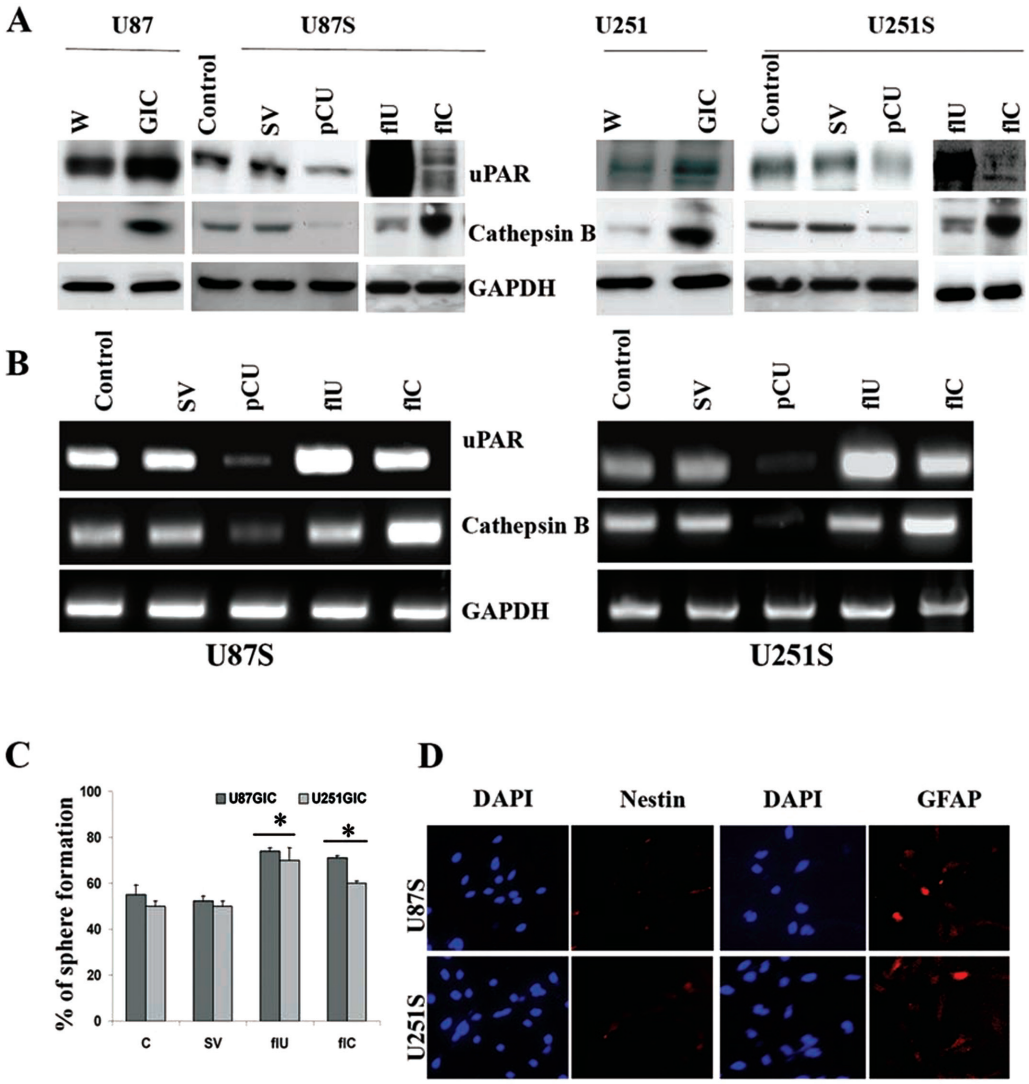

Fig. 2. uPAR and cathepsin B expression influence the self-renewal capacity of GICs. (**A**) Immunoblot analysis to determine the expression of uPAR and cathepsin B in wild-type and GICs. We also checked the efficiency of pCU, flU and flC transfection. Equal amounts of total protein were loaded; GAPDH was used as a loading control. (**B**) Total RNA isolated using Trizol reagent was subjected to RT–PCR analysis to determine the expression of uPAR and cathepsin B in U87S and U251S cells. GAPDH was used as a loading control. (**C**) Graphical representation of sphere forming ability (%) after flU and flC treatments. Data represented are averages of three different experiments (*$P \leq 0.05$). (**D**) Immunocyto analysis for the expression of Nestin and GFAP after transfecting U87S and U251 cells with pCU.

transcription (RT)–PCR analysis results indicated efficient downregulation of uPAR and cathepsin B with pCU treatment and a significant upregulation of both uPAR and cathepsin B with flU and flC treatments, respectively (Figure 2A and B). After flU and flC treatments, we observed an increased sphere-forming ability (an efficient indicator of self-renewal) in GICs (Figure 2C). In contrast, pCU treatment induced apoptosis with increased incubation time, and hence, we were unable to continue the experiments with pCU treatment in regards to the sphere formation assay. Next, to examine the expression of neural precursor or differentiation markers in cells, spheres in serum-free medium were disaggregated and seeded on poly-L-ornithine and fibronectin-coated glass slides. Downregulation of uPAR and cathepsin B decreased the number of cells positive for Nestin (a neural precursor cell marker) and increased the number of cells positive for GFAP (an astrocyte differentiated marker) (Figure 2D). Taken together, these findings suggest endogenous uPAR and cathepsin B signaling maintains the stemness of GICs.

uPAR and cathepsin B induce Sox2 and Bmi1 expression in GICs to maintain their stemness

To elucidate the mechanism by which the stemness of GICs is maintained by uPAR and cathepsin B, we next examined the effect of downregulation and upregulation of these two proteins on expression of various markers for stemness. Immunoblot analysis revealed decreased expression of Sox2 and Bmi1 in pCU-treated cell lysates, whereas we observed increased expression with the upregulation of uPAR and cathepsin B (Figure 3A).

To specify the roles of Sox2 and Bmi1 in inducing self-renewal, we used siRNA against Sox2 and Bmi1. The siRNA constructs efficiently downregulated the expression of Sox2 and Bmi1 in CD133+ cells (Figure 3B). Knockdown of Sox2 and Bmi1 expression by siRNA resulted in decreased size of CD133+ subpopulation (75.1–29.3% or 35.9% in both cell lines used) (Figure 3C) and drastic reduction of sphere-forming ability and self-renewal capacity of GICs (Figure 3D). These findings indicate that Sox2 and Bmi1 are essential for maintenance of stemness of GICs. To further confirm the role of uPAR and cathepsin B in upregulating Sox2 and Bmi1 expression, we created Bmi-promoter-luc and Sox2-promoter-luc constructs. After transfecting the cells with flU, flC and pCU, we carried out a second transfection with the luc constructs. Expression of luciferase under the control of Sox2 promoter increased by 2-fold in flU- and flC-transfected cells. However, pCU-transfected cells showed a 1.5-fold decrease in luciferase expression. Similarly, Bmi promoter driven luciferase construct

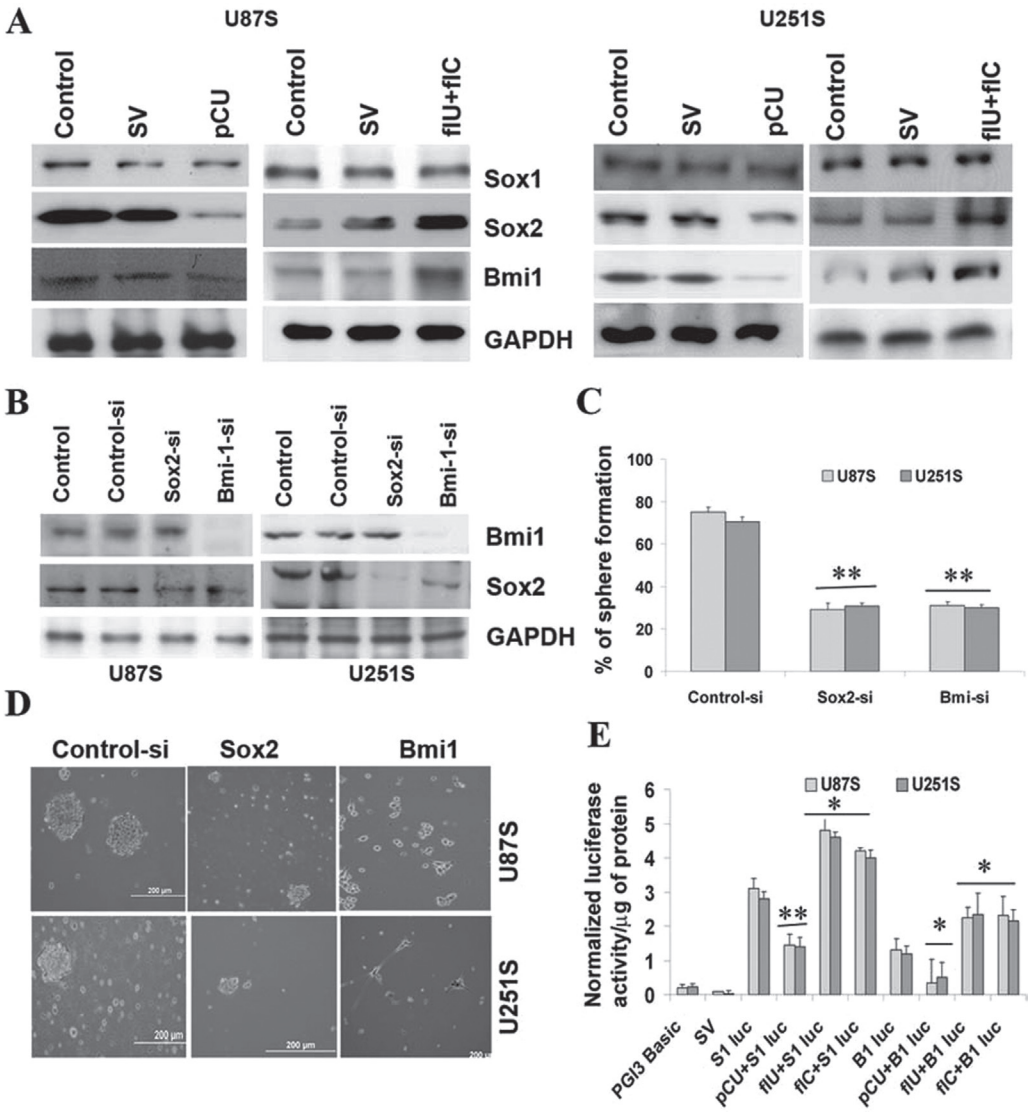

Fig. 3. Downregulation of uPAR and cathepsin B decreases the expression of Sox2 and Bmi1. (**A**) Immunoblot analysis to determine the expression of Sox1, Sox2 and Bmi1 after transfection of U87S and U251S cells with SV, pCU, flU and flC. (**B**) Total protein isolated from U87S and U251S cells transfected with Sox2-si and Bmi1-si was subjected to immunoblot analysis for determination of the expression of Sox2 and Bmi1. GAPDH was used as a loading control. (**C**) Graphical representation of sphere forming capacity of control siRNA, Sox-2-si and Bmi1-si-treated U87S and U251S cells (**$P \leq 0.01$). (**D**) Phase contrast pictures showing the decreased size of spheres after transfection with Sox-2-si and Bmi1-si. (**E**) U87S and U251S cells were initially transfected with SV, pCU, flU and flC. After 24 h of transfection, a second transfection was performed with S1-luc and Bmi1-luc constructs as described in Materials and methods. Luciferase expression was quantified using Promega's luciferase assay kit with a Turner Luminometer and is represented graphically. Luciferase expression after the various treatments is represented graphically (*$P \leq 0.05$, **$P \leq 0.01$).

showed a 1-fold increase in flU- and flC-treated cells compared with controls, and pCU-transfected cells showed a 1-fold decrease in luciferase expression compared with control in both the cell lines used. These results clearly show that uPAR and cathepsin B influence the expression of Sox2 and Bmi1 (Figure 3E).

Hedgehog signaling acts upstream of Sox2 and Bmi1

We compared expression of the genes in the hedgehog pathway in U87S and U251S to that of their wild-type cells. From quantitative RT–PCR analysis, we found that hedgehog receptors PTCH and SMO are expressed in both cell populations. However, GICs of both the cell lines expressed 4-fold higher levels of PTCH messenger RNA (mRNA) and 3-fold higher levels of SMO mRNA than wild-type glioma cells. We measured the expression of transcription factors GLI1 and GLI2, which are downstream components of the hedgehog pathway, and found that GICs have almost 10-fold higher levels of GLI1 mRNA and 6-fold higher levels of GLI2 mRNA than wild-type cells (Figure 4A). Taken together, these results indicate that the hedgehog signaling pathway is activated in stem/progenitor cells.

We next checked the effect of uPAR and cathepsin B upregulation and downregulation on hedgehog signaling components. The simultaneous downregulation of uPAR and cathepsin B reduced the expression of GLI1 and GLI2 and increased PTCH at the RNA level and *vice versa* in uPAR- and cathepsin B-upregulated cells (Figure 4B). To confirm that uPAR and cathepsin B affected GLI2 expression, we constructed a 2.0 kb GLI2-luc–pGL3 vector and determined luciferase expression after treatment. Luciferase expression increased by 2-fold in flU- and flC-treated cells but decreased by 2.5-fold in pCU-treated cells as compared with cells transfected with GLI2-luc alone (Figure 4C). To determine whether uPAR- and cathepsin B-mediated high expression of Sox2 and Bmi1 occurs through hedgehog signaling, we used cyclopamine (10 μM) in this study. When treated with cyclopamine, U251S and U87S cells showed decreased expression of GLI2 at the RNA level. Real-time PCR data showed a 3-fold decrease of GLI2 levels in both cell lines (Figure 4D).

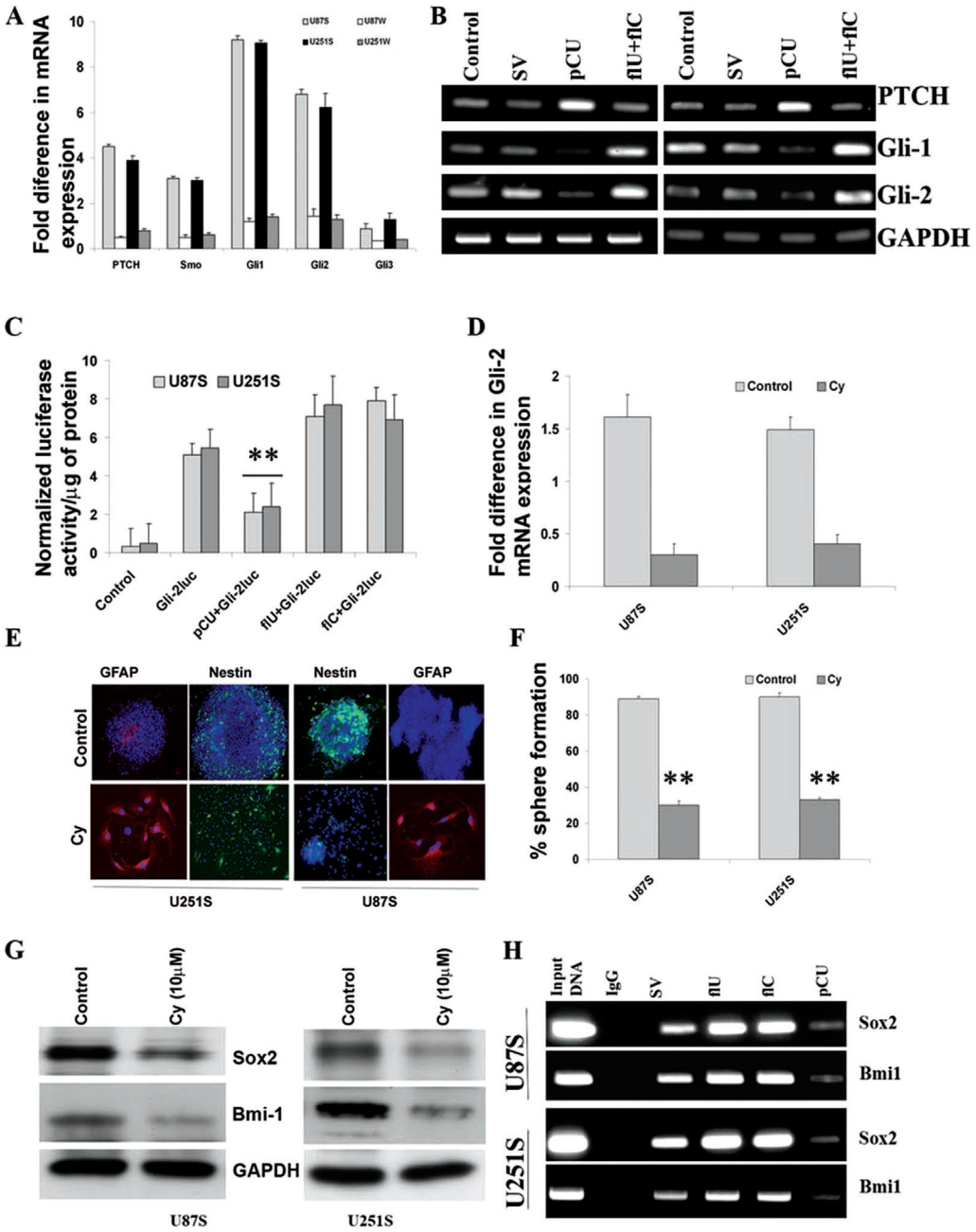

Fig. 4. Hedgehog signaling acts upstream of Sox2 and Bmi1. (**A**) Real-time PCR analysis of hedgehog signaling molecules such as PTCH, SMO, GLI1, GLI2 and GLI3 in U87S, U251S, U87W and U251W cells. (**B**) RT–PCR analysis for the expression levels of PTCH, GLI1 and GLI2 at the mRNA level after transfection with SV, pCU, flU and flC. GAPDH was used as a loading control. (**C**) Graphical representation of luciferase expression obtained after transfection with pCU, flU, flC and GLI2-luc constructs (*$P \leq 0.05$, **$P \leq 0.01$). (**D**) Influence of cyclopamine (10 μM) treatment on the expression of GLI2 at the mRNA level. Total RNA was isolated from U87S and U251S cells after 24 h of cyclopamine treatment and subjected to RT–PCR analysis. Fold difference in the expression of GLI2 is represented graphically. (**E**) Immunocyto analysis to check the effect of cyclopamine on differentiation and the expression of stem cell markers. Immunocyto analysis was performed for GFAP and Nestin expression after cyclopamine treatment. Overlapped pictures of DAPI and the specified antibody are represented. (**F**) Graphical representation of sphere forming ability after cyclopamine treatment is represented (**$P \leq 0.01$). (**G**) Effect of cyclopamine treatment on Sox2 and Bmi1 expression. Immunoblot analysis of total protein was performed for Sox2 and Bmi1 expression. GAPDH was used as a loading control. (**H**) Nuclear extracts isolated from U87S and U251S cells were subjected to chromatin immunoprecipitation analysis. GLI2 immunoprecipitations were carried out, and the co-precipitated chromatin was analyzed using PCR with specific primers for the Sox2 and Bmi1 promoter sequence.

Also, when treated with cyclopamine in two-well chamber slides, the spheres showed increased differentiation of cells from spheres. In addition, the differentiated cells showed high expression of the differentiation marker GFAP and decreased expression of Nestin (Figure 4E). The smaller spheres in the treated wells completely differentiated and those pictures are represented. When treated with cyclopamine, dissociated GIC cells generated 20% secondary sphere formation as compared with 80% in untreated cells (Figure 4F). Further, immunoblot analysis of the cells treated with cyclopamine, a specific hedgehog inhibitor, showed decreased expression of Sox2 and Bmi1, which indicates that hedgehog signaling might act upstream of Sox2 and Bmi1 (Figure 4G).

uPAR and cathepsin B overexpression increases GLI binding on Sox2 and Bmi1 promoters

As indicated by the earlier experiments, cyclopamine treatment decreased expression of Sox2 and Bmi1. To examine whether this

regulation is direct, we performed chromatin immunoprecipitation assay using antibody against GLI2. PCR amplification of chromatin DNA cross-linked to GLI2 showed the presence of Sox2 and Bmi1 promoter fragments spanning the regions between −341 to −643 and −92 to −234, respectively, in control cells suggesting binding by endogenous GLI2. Recruitment of GLI2 to the Sox2 and Bmi1 promoters increased 48 h after flU and flC treatments of U87S and U251S cells; this recruitment was clearly suppressed by pCU treatment (Figure 4H). These results appear to be due to regulation of Sox2 and Bmi1 by the GLI transcription factors.

Irradiation-induced uPAR and cathepsin B are involved in the maintenance of the stem cell nature of GICs

As radiation is known to be involved in increasing stem cell properties of various cancers, we checked whether uPAR and cathepsin B play roles in irradiation-induced stem cell marker expression. Initially, we checked the effect of radiation alone on uPAR, cathepsin B, CD133, Sox2 and Bmi1 expression. Immunoblot analysis revealed that increased radiation dosage (5 and 10 Gy) induced the expression of all of the above-mentioned molecules (Figure 5A). Further, when the irradiation-induced uPAR and cathepsin B expression was downregulated with pCU treatment, the expression levels of irradiation-induced CD133, Sox2 and Bmi1 were decreased (Figure 5B) and the upregulation of these proteins was by the percentage increase of high

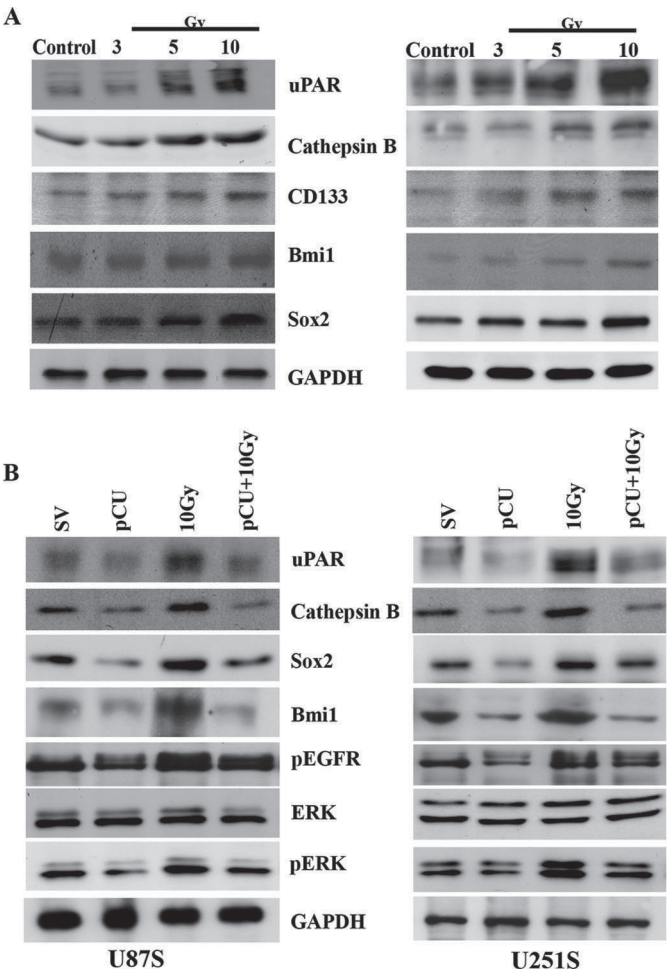

Fig. 5. Downregulation of uPAR and cathepsin B decreased the expression of irradiation-induced stem cell-related proteins. (**A**) Effect of different doses of radiation on the expression of uPAR, cathepsin B, CD133, Bmi1 and Sox2. Total protein isolated after 48 h of radiation was subjected to immunoblot analysis. GAPDH was used as a loading control. (**B**) Effect of downregulation of uPAR and cathepsin B on irradiation-induced Sox2 and Bmi1 expression.

expression of cell population (data not shown). These results indicate that the expression of irradiation-induced stemness-related proteins is at least partially controlled by uPAR and cathepsin B.

Downregulation of uPAR and cathepsin B suppresses expression of Sox2, Bmi1 and Nestin in vivo

We studied the effect of RNAi-mediated inhibition of cathepsin B and uPAR on pre-established tumors. Hematoxylin and eosin staining revealed a large spread of tumor growth in mock and SV-treated brain sections of U87S and U251S cells (Figure 6A). pCU treatment increased the survival of mice compared with the controls (Figure 6B). Immunohistochemical analysis of the tumor sections from control and SV-treated mice for cathepsin B and uPAR showed increased expression levels localized to the tumor region, whereas pCU-treated tumor sections revealed very little or no expression of cathepsin B and uPAR. When probed for Sox2, Bmi1 and CD133 protein expression, mock and SV-treated brain sections showed very high expression levels, whereas pCU-treated brain sections showed low expression (Figure 6C), indicating that stem cell-related molecules are efficiently inhibited by the downregulation of uPAR and cathepsin B.

Discussion

Cancer-initiating cells comprise a heterogeneous population of undifferentiated cells with the capacity for self-renewal and a high proliferative potential. Any potential cancer therapy must also target the cancer-initiating cells to successfully eradicate tumors (42). The property of self-renewal is unique to stem cells. To investigate the role of uPAR and cathepsin B in the maintenance of stem cell nature, we used full-length complementary DNA clones to overexpress uPAR and cathepsin B and a bicistronic construct with shRNA against uPAR and cathepsin B in this study. Here, we have shown that components of uPAR and cathepsin B are important in maintenance of stem cells and are highly expressed in GICs. Furthermore, we show that upregulation of uPAR and cathepsin B promotes self-renewal of GICs through increased expression of hedgehog signaling components and high expression of Sox2 and Bmi1. Finally, we demonstrate that Sox2 and Bmi1 act downstream of hedgehog signaling as reflected by their inhibition with cyclopamine, a specific inhibitor of the hedgehog pathway.

Sox2 is known to be an important self-renewal gene and plays a pivotal role in maintaining stemness of embryonic stem cells (43) and NSCs (44). In glioma cells, expression levels of Sox2 are linearly and exponentially correlated with those of Nestin and CD133, respectively (45). Although it has been reported that glioma tissues highly express Sox2 mRNA as compared with non-malignant tissues (20,46), the role of Sox2 in glioma development has not yet been determined. Also, it has recently been reported that the polycomb gene *Bmi1* plays an important role in the regulation of self-renewal of hematopoietic (47) and neuronal stem cells (34). Here, we have shown that Sox2 and Bmi1 are expressed at increased levels in GICs when compared with wild-type U87 and U251 glioma cells. Their expression levels increased with uPAR and cathepsin B upregulation and *vice versa* with shRNA treatments. Furthermore, uPAR and cathepsin B upregulation increased the self-renewal capacity of U87 and U251 GICs as observed by the increased size of glioma spheres and increased subsphere formation *in vitro*. Thus, siRNA targeted against Sox2 and Bmi1 significantly reduced the self-renewal capacity of GICs, which indicates that uPAR and cathepsin B play important roles in self-renewal of GICs via Sox2 and Bmi1.

Independent studies have demonstrated that hedgehog signaling regulates Bmi1 expression in various cancers including glioma (48). Similarly, GLI2 has been reported to be a novel regulator of Sox2 in neuroepithelial cells (49). Hence, we studied the effect of uPAR and cathepsin B upregulation and downregulation on the expression of hedgehog signaling components. GLI1 and GLI2 are positive mediators of hedgehog signaling, whereas GLI3 functions as a negative regulator of this pathway (50,51). Consequently, we focused only on GLI1 and GLI2 in this study. Interestingly, we

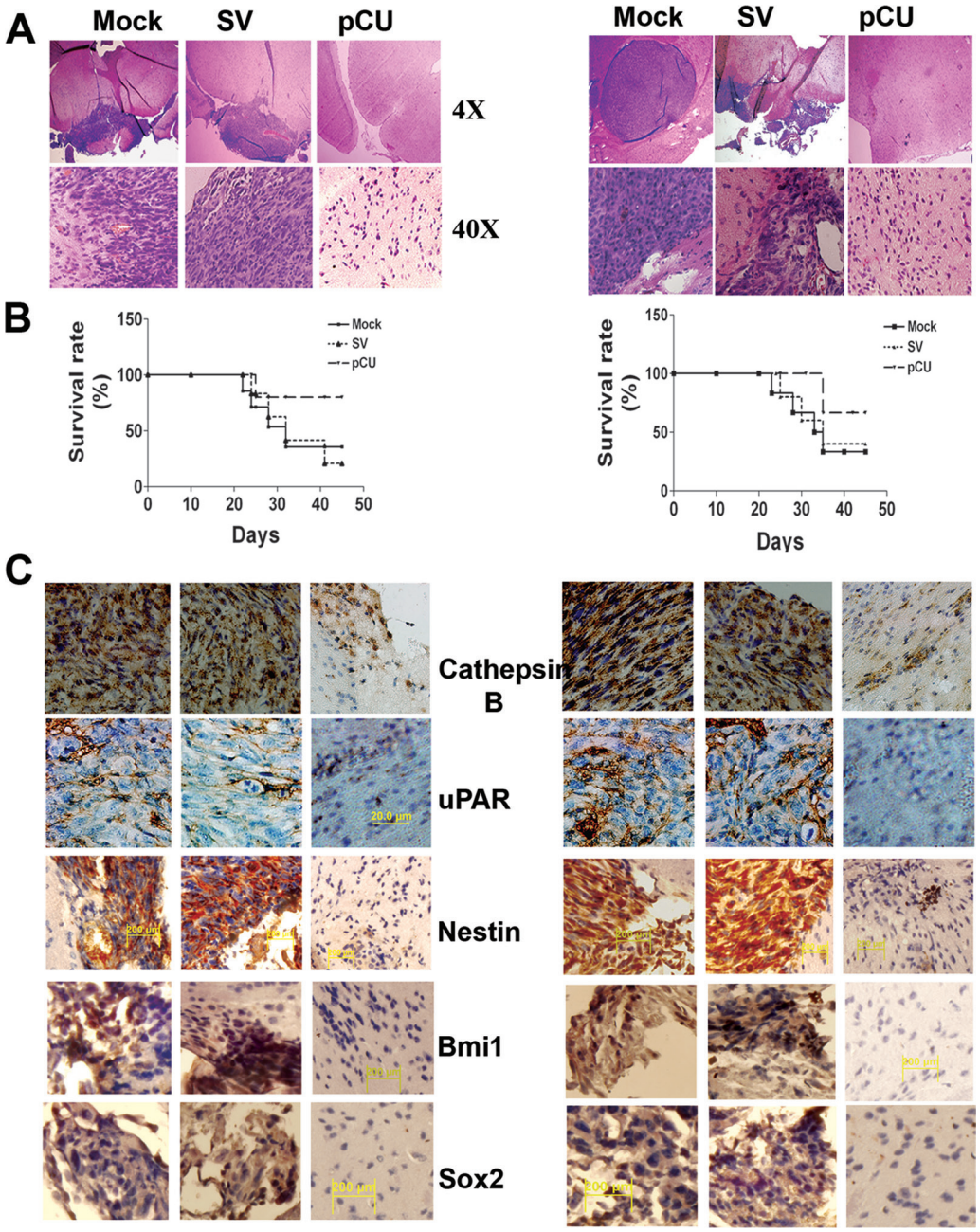

Fig. 6. Downregulation of cathepsin B and uPAR suppresses tumor growth and decreases stem cell marker expression *in vivo*. Stereotactic implantation of U87S and U251S tumor cells was carried out. After 1 week, PBS (mock), SV or pCU was injected into the brain using an Alzet mini-osmotic pump. Five animals per group were used. Thirty days after implantation, the animals were killed, the brains were removed and fixed, and paraffin sections were prepared. (**A**) Hematoxylin and eosin staining of tissue sections to visualize tumor cells and to examine tumor volumes. (**B**) Survival as evaluated by Kaplan–Meier analysis (5 mice per group). (**C**) Immunohistochemical analysis of uPAR, cathepsin B, Nestin, Sox2 and Bmi1 in paraffin-embedded tissue sections.

observed a significant increase in GLI2 transcription factor when uPAR and cathepsin B were upregulated and *vice versa* with pCU treatment. Decreased protein expression of Sox2 and Bmi1 and decreased luciferase expression of S1-luc and B1 luc with the cyclopamine treatment further confirmed that GLI2 acts upstream of Sox2 and Bmi1. Chromatin immunoprecipitation analysis proved that GLI2 binds to both Sox2 and Bmi1 promoters and strongly suggests that GLI2 directly acts on Sox2 and Bmi1. Takanaga *et al.* (49) has reported that GLI2 binds to an enhancer that is vital for Sox2 expression, and a mechanism has been proposed that Sox2 maintains the undifferentiated state of neural stem cells through the GLI2-Sox2-Hes5 signal cascade. More recently, Gangemi *et al.* (18) showed that silencing of Sox2 in freshly derived GBM tumor-initiating cells stopped proliferation, and the resulting cells lost tumorigenicity in immunodeficient mice. Ikushima *et al.* (19) showed that inhibition of transforming growth factor-β signaling drastically decreased the tumorigenicity of GICs by promoting their differentiation, and that these effects were attenuated in GICs transduced with Sox2 or Sox4. Further, radiation induced expression of Bmi1 and Sox2, and increased phospho protein levels of ERK and EGFR were significantly decreased when treated with pCU. Eberl *et al.* (52) described that HH-EGFR cooperation response genes including SOX2, SOX9, JUN, CXCR4 and FGF19 were synergistically activated by HH-EGFR signal integration and were required for *in vivo* growth of BCC cells and tumor-initiating pancreatic cancer cells. Similarly, synergistic interaction of EGFR/

MEK/ERK and GLI2-induced oncogenic transformation has been reported (53). Thus, the findings of this study indicate that uPAR and cathepsin B regulates the self-renewal capacity of GICs.

In vivo results showed that the GICs had higher tumorigenic capacity when the cells were injected intracranially. However, CD133– cells (1×10^4) showed no signs of tumor within the specified period of time. These results indicate that populations with a higher tumorigenic activity were enriched in 'sphere' cells. In this study, immunohistochemistry revealed that along with cathepsin B and uPAR, the expression of Sox2, Bmi1 and GLI1 were also decreased in pCU-treated brain sections as compared with controls. Given the high degree of drug resistance and the shared cellular and gene expression profiles of adult and cancer stem cells (46), targeting cancer stem cells (CSC) has proven to be difficult. However, decreasing self-renewal capacity and/or inducing differentiation/apoptosis remain a promising therapeutic strategy for cancer stem cells. Piccirillo *et al*. (54)showed that bone morphogenetic proteins can induce differentiation of CD133+ GBM cells, thereby reducing their tumorigenic potential. The overexpression of a truncated form of GLI2 (GLI2_C) or *GLI2*-specific shRNA *in vivo* and *in vitro* inhibits cell proliferation and the expression of Sox2 and other NSC markers, including CD133, and Bmi1 in telencephalic neuroepithelial cells (49). To our knowledge, our report is the first to show the significance of uPAR and cathepsin B in maintenance of self-renewal of GICs. Our results highlight the importance of uPAR and cathepsin B in the regulation of malignant stem cell self-renewal through hedgehog pathway components, Bmi1 and Sox2, and suggest that strategies aimed at inhibiting uPAR and cathepsin B represent a rational therapeutic approach to target cancer stem cells. Taken together, these results lend support to the cancer stem cell hypothesis.

Supplementary material

Supplementary Table 1 and Figures 1 and 2 can be found at http://carcin.oxfordjournals.org/

Funding

National Institute of Health (#CA116708).

Acknowledgements

We thank Peggy Mankin and Noorjehan Ali for technical assistance, Susan Renner for manuscript preparation, and Diana Meister and Sushma Jasti for manuscript review.
The contents are solely the responsibility of the authors and do not necessarily represent the official views of NIH. The funders had no role in the design of the study, data collection and analysis, decision to publish, or preparation of the manuscript.

Conflict of Interest Statement: None declared.

References

1. Louis,D.N. *et al.* (2007) The 2007 WHO classification of tumours of the central nervous system. *Acta Neuropathol.*, **114**, 97–109.
2. Deorah,S. *et al.* (2006) Trends in brain cancer incidence and survival in the United States: Surveillance, Epidemiology, and End Results Program, 1973 to 2001. *Neurosurg. Focus*, **20**, E1.
3. Galli,R. *et al.* (2004) Isolation and characterization of tumorigenic, stem-like neural precursors from human glioblastoma. *Cancer Res.*, **64**, 7011–7021.
4. Singh,S.K. *et al.* (2003) Identification of a cancer stem cell in human brain tumors. *Cancer Res.*, **63**, 5821–5828.
5. Singh,S.K. *et al.* (2004) Identification of human brain tumour initiating cells. *Nature*, **432**, 396–401.
6. Dontu,G. *et al.* (2003) Stem cells in normal breast development and breast cancer. *Cell Prolif.*, **36** (suppl 1), 59–72.
7. Kopper,L. *et al.* (2004) Tumor stem cells. *Pathol. Oncol. Res.*, **10**, 69–73.
8. Taipale,J. *et al.* (2001) The Hedgehog and Wnt signalling pathways in cancer. *Nature*, **411**, 349–354.
9. Leis,O. *et al.* (2012) Sox2 expression in breast tumours and activation in breast cancer stem cells. *Oncogene*, **31**, 1354–1365.
10. Nakatsugawa,M. *et al.* (2011) SOX2 is overexpressed in stem-like cells of human lung adenocarcinoma and augments the tumorigenicity. *Lab Invest.*, **91**, 1796–1804.
11. Park,I.K. *et al.* (2004) Bmi1, stem cells, and senescence regulation. *J. Clin. Invest.*, **113**, 175–179.
12. Dahmane,N. *et al.* (2001) The Sonic Hedgehog-Gli pathway regulates dorsal brain growth and tumorigenesis. *Development*, **128**, 5201–5212.
13. Clement,V. *et al.* (2007) HEDGEHOG-GLI1 signaling regulates human glioma growth, cancer stem cell self-renewal, and tumorigenicity. *Curr. Biol.*, **17**, 165–172.
14. Ehtesham,M. *et al.* (2007) Ligand-dependent activation of the hedgehog pathway in glioma progenitor cells. *Oncogene*, **26**, 5752–5761.
15. Fong,H. *et al.* (2008) Regulation of self-renewal and pluripotency by Sox2 in human embryonic stem cells. *Stem Cells*, **26**, 1931–1938.
16. Masui,S. *et al.* (2007) Pluripotency governed by Sox2 via regulation of Oct3/4 expression in mouse embryonic stem cells. *Nat. Cell Biol.*, **9**, 625–635.
17. Suh,H. *et al.* (2007) *In vivo* fate analysis reveals the multipotent and self-renewal capacities of Sox2+ neural stem cells in the adult hippocampus. *Cell Stem Cell*, **1**, 515–528.
18. Gangemi,R.M. *et al.* (2009) SOX2 silencing in glioblastoma tumor-initiating cells causes stop of proliferation and loss of tumorigenicity. *Stem Cells*, **27**, 40–48.
19. Ikushima,H. *et al.* (2009) Autocrine TGF-beta signaling maintains tumorigenicity of glioma-initiating cells through Sry-related HMG-box factors. *Cell Stem Cell*, **5**, 504–514.
20. Schmitz,M. *et al.* (2007) Identification of SOX2 as a novel glioma-associated antigen and potential target for T cell-based immunotherapy. *Br. J. Cancer*, **96**, 1293–1301.
21. Park,E.T. *et al.* (2008) Aberrant expression of SOX2 upregulates MUC5AC gastric foveolar mucin in mucinous cancers of the colorectum and related lesions. *Int. J. Cancer*, **122**, 1253–1260.
22. Chen,Y. *et al.* (2008) The molecular mechanism governing the oncogenic potential of SOX2 in breast cancer. *J. Biol. Chem.*, **283**, 17969–17978.
23. Sanada,Y. *et al.* (2006) Histopathologic evaluation of stepwise progression of pancreatic carcinoma with immunohistochemical analysis of gastric epithelial transcription factor SOX2: comparison of expression patterns between invasive components and cancerous or nonneoplastic intraductal components. *Pancreas*, **32**, 164–170.
24. Ferri,A.L. *et al.* (2004) Sox2 deficiency causes neurodegeneration and impaired neurogenesis in the adult mouse brain. *Development*, **131**, 3805–3819.
25. Annovazzi,L. *et al.* (2011) SOX2 expression and amplification in gliomas and glioma cell lines. *Cancer Genomics Proteomics*, **8**, 139–147.
26. Leung,C. *et al.* (2004) Bmi1 is essential for cerebellar development and is overexpressed in human medulloblastomas. *Nature*, **428**, 337–341.
27. Vonlanthen,S. *et al.* (2001) The bmi-1 oncoprotein is differentially expressed in non-small cell lung cancer and correlates with INK4A-ARF locus expression. *Br. J. Cancer*, **84**, 1372–1376.
28. Kim,T.Y. *et al.* (2006) Epigenomic profiling reveals novel and frequent targets of aberrant DNA methylation-mediated silencing in malignant glioma. *Cancer Res.*, **66**, 7490–7501.
29. Haupt,Y. *et al.* (1993) bmi-1 transgene induces lymphomas and collaborates with myc in tumorigenesis. *Oncogene*, **8**, 3161–3164.
30. Matsui,W. *et al.* (2004) Characterization of clonogenic multiple myeloma cells. *Blood*, **103**, 2332–2336.
31. Nowak,K. *et al.* (2006) BMI1 is a target gene of E2F-1 and is strongly expressed in primary neuroblastomas. *Nucleic Acids Res.*, **34**, 1745–1754.
32. Godlewski,J. *et al.* (2008) Targeting of the Bmi-1 oncogene/stem cell renewal factor by microRNA-128 inhibits glioma proliferation and self-renewal. *Cancer Res.*, **68**, 9125–9130.
33. Bruggeman,S.W. *et al.* (2005) Ink4a and Arf differentially affect cell proliferation and neural stem cell self-renewal in Bmi1-deficient mice. *Genes Dev.*, **19**, 1438–1443.
34. Molofsky,A.V. *et al.* (2003) Bmi-1 dependence distinguishes neural stem cell self-renewal from progenitor proliferation. *Nature*, **425**, 962–967.
35. Molofsky,A.V. *et al.* (2005) Bmi-1 promotes neural stem cell self-renewal and neural development but not mouse growth and survival by repressing the p16Ink4a and p19Arf senescence pathways. *Genes Dev.*, **19**, 1432–1437.
36. Zencak,D. *et al.* (2005) Bmi1 loss produces an increase in astroglial cells and a decrease in neural stem cell population and proliferation. *J. Neurosci.*, **25**, 5774–5783.
37. Valk-Lingbeek,M.E. *et al.* (2004) Stem cells and cancer; the polycomb connection. *Cell*, **118**, 409–418.
38. Gondi,C.S. *et al.* (2006) RNA interference-mediated simultaneous down-regulation of urokinase-type plasminogen activator receptor and cathepsin

B induces caspase-8-mediated apoptosis in SNB19 human glioma cells. *Mol. Cancer Ther.*, **5**, 3197–3208.
39. Gondi,C.S. *et al.* (2007) Intraperitoneal injection of a hairpin RNA-expressing plasmid targeting urokinase-type plasminogen activator (uPA) receptor and uPA retards angiogenesis and inhibits intracranial tumor growth in nude mice. *Clin. Cancer Res.*, **13**, 4051–4060.
40. Lakka,S.S. *et al.* (2004) Inhibition of cathepsin B and MMP-9 gene expression in glioblastoma cell line via RNA interference reduces tumor cell invasion, tumor growth and angiogenesis. *Oncogene*, **23**, 4681–4689.
41. Hemmati,H.D. *et al.* (2003) Cancerous stem cells can arise from pediatric brain tumors. *Proc. Natl. Acad. Sci. U.S.A.*, **100**, 15178–15183.
42. Dingli,D. *et al.* (2006) Successful therapy must eradicate cancer stem cells. *Stem Cells*, **24**, 2603–2610.
43. Kamachi,Y. *et al.* (2000) Pairing SOX off: with partners in the regulation of embryonic development. *Trends Genet.*, **16**, 182–187.
44. Graham,V. *et al.* (2003) SOX2 functions to maintain neural progenitor identity. *Neuron*, **39**, 749–765.
45. Lee,J. *et al.* (2006) Tumor stem cells derived from glioblastomas cultured in bFGF and EGF more closely mirror the phenotype and genotype of primary tumors than do serum-cultured cell lines. *Cancer Cell*, **9**, 391–403.
46. Ben-Porath,I. *et al.* (2008) An embryonic stem cell-like gene expression signature in poorly differentiated aggressive human tumors. *Nat. Genet.*, **40**, 499–507.
47. Park,I.K. *et al.* (2003) Bmi-1 is required for maintenance of adult self-renewing haematopoietic stem cells. *Nature*, **423**, 302–305.
48. Liu,S. *et al.* (2006) Hedgehog signaling and Bmi-1 regulate self-renewal of normal and malignant human mammary stem cells. *Cancer Res.*, **66**, 6063–6071.
49. Takanaga,H. *et al.* (2009) Gli2 is a novel regulator of sox2 expression in telencephalic neuroepithelial cells. *Stem Cells*, **27**, 165–174.
50. Hwang,Y.S. *et al.* (1992) Efficacy of once-daily felodipine monotherapy in systemic hypertension. *Am. J. Cardiol.*, **69**, 271–274.
51. Stecca,B. *et al.* (2005) Interference with HH-GLI signaling inhibits prostate cancer. *Trends Mol. Med.*, **11**, 199–203.
52. Eberl,M. *et al.* (2012) Hedgehog-EGFR cooperation response genes determine the oncogenic phenotype of basal cell carcinoma and tumour-initiating pancreatic cancer cells. *EMBO Mol. Med.*, **4**, 218–233.
53. Schnidar,H. *et al.* (2009) Epidermal growth factor receptor signaling synergizes with Hedgehog/GLI in oncogenic transformation via activation of the MEK/ERK/JUN pathway. *Cancer Res.*, **69**, 1284–1292.
54. Piccirillo,S.G. *et al.* (2006) Bone morphogenetic proteins regulate tumorigenicity in human glioblastoma stem cells. *Ernst. Schering. Found. Symp. Proc.,* **5**, 59–81.

Received May 2, 2012; revised October 26, 2012; accepted November 22, 2012